Facial Bone Scanning by Emission Tomography

Manuel L. Brown*, John W. Keyes, Jr., Patrick F. Leonard,
James H. Thrall, and Louis T. Kircos

University of Michigan Medical Center, Ann Arbor, Michigan

A single-photon emission tomographic system was used to study the normal anatomy of the facial bones and the usefulness of emission computed tomography in evaluating diseases of the bones of the face. The examination was performed following routine bone scintigraphy and took an additional 20–30 min. The anatomy of the facial bones was well defined, with clear separation of deep and superficial structures. Early experience with tumor, infection, bone grafts, and postirradiation osteonecrosis indicates that useful added diagnostic information can be obtained by this method.

J Nucl Med 18: 1184–1188, 1977

The bone scan is a useful procedure for identifying and locating disease in all parts of the skeleton. In the axial and appendicular skeleton, the demonstration of abnormal areas is easily accomplished by anterior and posterior views and occasionally lateral views. This is not the case in the facial region. The anatomy of the facial bones is complex and numerous structures overlap, making accurate location of abnormalities by bone scanning extremely difficult. Gates and Goris (*1*) correctly point out the need for multiple projections to aid in accurate location of disease processes. Even with multiple projections, overlapping structures may not allow adequate separation of normal and abnormal areas. The use of a technique such as computed tomography, which provides for the separation of structures in three dimensions, should help to overcome these difficulties. This study was undertaken to define the normal anatomy of the facial bones by emission computed tomography (ECT) and to evaluate in a preliminary fashion the usefulness of this technique in diseases involving the bones of the face.

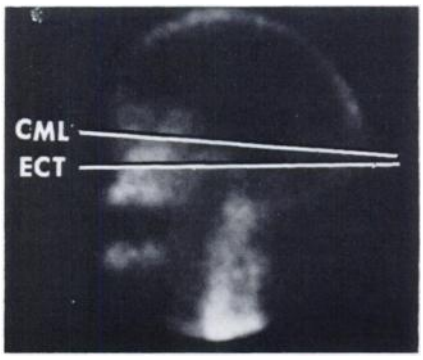

FIG. 1. Relationship of canthomeatal line to plane of reconstructions presented in this paper. (CML) canthomeatal line; (ECT) plane in emission computed tomography.

MATERIALS AND METHODS

Patients were studied 3 to 4 hr after administration of 15 mCi of Tc-99m pyrophosphate. Emission computed tomography of the face and head was performed with a single-photon emission tomographic system, the Humongotron, a system described by Keyes et al. (*2*). A high-resolution parallel-hole collimator was used, and total time for tomographic data acquisition was between 20 and 30 min.

Serial transaxial tomographic reconstructions corresponding to 12-mm-thick sections were made of all levels of the head and face from the vertex to below the mandible. Data-processing time was approximately 30 sec per reconstruction using a filtered back-projection algorithm without correction for attenuation. Between 8 and 12 sections were usually required to reconstruct the entire volume of the face.

Received June 23, 1977; revision accepted Aug. 4, 1977.

For reprints contact: Manuel Brown, Mayo Clinic, Rochester, MN 55501.

* Current Address: Mayo Clinic, Rochester, MN 55501.

Six patients without clinical, radiographic, or scan evidence of head and neck disease provided samples of normal anatomy. The reconstructed sections were carefully compared with skulls and transverse sections of the head provided by the University of Michigan Department of Anatomy, and with several standard textbooks and atlases of cross-sectional anatomy (*3–5*).

Eight patients with various disease processes involving the face and jaw were also studied in order to provide correlation with the normal anatomy and to offer a preliminary basis for judging the clinical utility of the technique. The diseases studied included sinusitis, osteoradionecrosis, osteomyelitis, bone grafts, and several different neoplasms.

RESULTS

In most cases the images demonstrated resolution comparable with that obtained in conventional gamma-camera images. Motion artefacts degraded some of the images, although in only one case was the study rendered uninterpretable. In all of the technically satisfactory studies the tomographic presentation was superior to conventional images in displaying the anatomy of the facial bones.

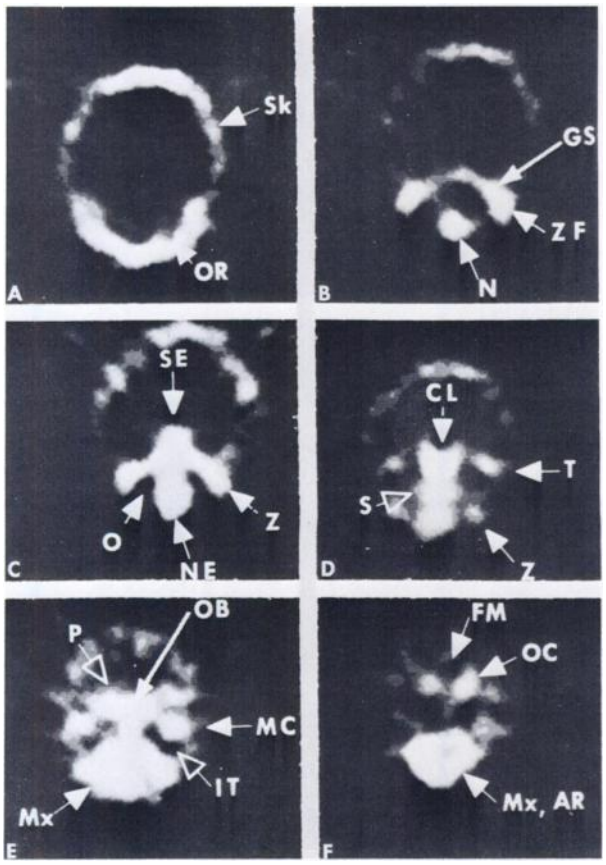

FIG. 2. Normal anatomy shown in contiguous sections extending from level of orbital roof and frontal sinus (A) downward to level of alveolar ridge of maxilla (F). These and all other sections shown are approximately 12 mm thick and oriented with subject's face toward bottom of figure and viewed from above. (Sk) skull; (OR) orbital roof; (GS) greater wing of sphenoid; (ZF) zygomatic-frontal process; (N) nasion; (SE) sella turcica; (O) orbit; (NE) naso-ethmoid region; (Z) zygomatic arch; (CL) clivus; (T) temporal bone; (S) body of sphenoid; (P) petrous pyramid; (OB) occipital bone; (MC) mandibular condyle; (IT) infratemporal fossa; (Mx) maxilla; (FM) foramen magnum; (OC) occipital condyle; (AR) alveolar ridge.

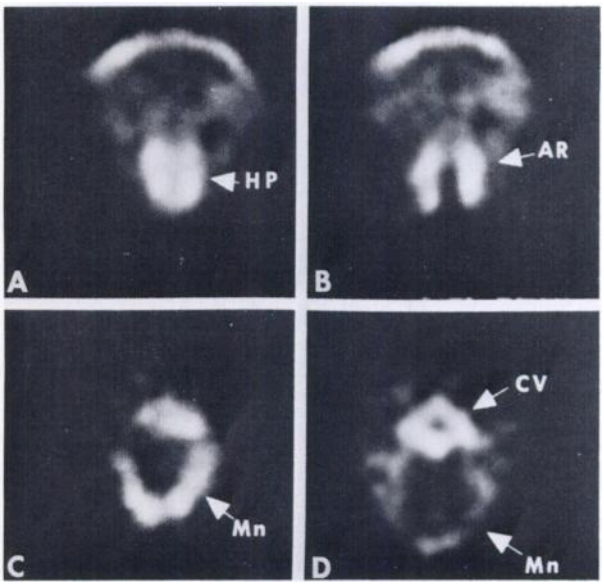

FIG. 3. Selected planes illustrating normal anatomy. (A) Level of hard palate; (B) level of alveolar ridge of maxilla; (C) level of mandible; (D) level of upper cervical spine with mandible distorted by partial volume artifact; (HP) hard palate; (AR) alveolar ridge; (Mn) mandible; (CV) cervical vertebra.

Normal anatomy. Due to constraints in patient positioning, the reconstructed sections are at a slight angle (10–15°) to the plane defined by the canthomeatal line (Fig. 1). Although this is not a significant shortcoming, it does make correlation with conventional transverse-section anatomy texts difficult, since the sections presented therein are invariably parallel to the canthomeatal line.

Normal anatomy as defined by ECT is depicted in Figs. 2 and 3. In these and all other reconstructions shown, the sections are viewed from above with the subject's face toward the bottom of the figure. The subject's right is thus on the viewer's left.

Representative case studies. *Case 1* (Fig. 4). A 45-year-old diabetic man had the chief complaint of a swollen left cheek 6 mo after the extraction of a molar. Radiographic exam showed a normal left maxillary sinus. Routine bone scan was normal. Tomography shows asymmetrical localization of tracer with greater uptake in the left maxilla and lower maxillary sinus than on the right. The discharge diagnosis was actinomycosis.

Case 2 (Fig. 5). A 49-year-old man had a 1-yr history of a mass in the right maxillary area following multiple dental extractions. Skull radiographs were

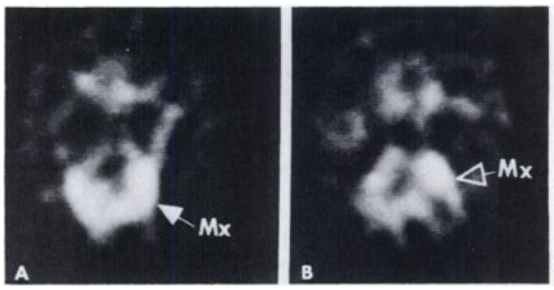

FIG. 4. Case 1. Actinomycosis: (A) level of alveolar ridge of maxilla showing increased uptake in left aveolar ridge at tip of arrow; (B) next higher section showing uptake in wall of maxillary sinus at tip of arrow. (Mx) maxilla.

normal. Sinus radiographs showed right maxillary antral mucosal thickening. The bone scan showed two discrete areas of increased tracer uptake over the right maxillary region and right frontal bone. Emission tomography clearly locates the process in the maxilla, zygoma, lateral wall of orbit, and frontal bone, extending almost to the vertex as one continuous area. Involvement of the body of the sphenoid is also clearly seen. Biopsy revealed histiocytic lymphoma.

Case 3 (Figs. 6 and 7). A 49-year-old man had failure of wound healing following tooth extractions. Physical exam revealed a firm fixed mass in the area of the right submandibular gland. Mandibular radiographs showed bone erosion. The bone scan showed possible increased tracer uptake in the right mandible. Emission tomography clearly shows a localized photon-deficient region surrounded by increased activity in the reactive bone. The pathologic diagnosis was a squamous-cell carcinoma infiltrating the mandible.

Case 4 (Fig. 8). A 50-year-old woman had undergone radiation therapy for a squamous-cell carcinoma of the floor of the mouth. She had developed postirradiation osteonecrosis of the left mandible. The clinical question was whether there was viable, perfused bone surrounding the necrotic focus. The emission scan showed the necrotic area with reactive bone both laterally and inferiorly, demonstrating that the remainder of the left jaw was viable and that healing was possible.

DISCUSSION

Relatively few authors have stressed bone scanning in patients with head and neck diseases. Arft (*6*) studied a series of patients with and without dental disease and showed that increased tracer uptake occurred after recent dental extraction and with early periapical disease. Garcia et al. (*7*) have also evaluated the use of bone imaging in dental disease and feel that it is of potential use in detecting incipient dental disease as well as in distinguishing active from arrested disease. Olson and McCombs (*8*) presented a case of ameloblastoma of the jaw with intense tracer localization, and Alexander et al. (*9*) reported using bone scans in the evaluation of patients with squamous-cell carcinoma, chondrosarcoma, multiple myeloma, fibrous dysplasia, cementifying fibroma, central giant-cell lesions, odontomas, osteomyelitis, bone grafts, and various dental cysts. They concluded that these conditions were detected earlier and more accurately with scintigraphy than with radiographs.

In order to interpret bone scans of the facial region adequately, a knowledge of normal anatomy is necessary. Jones and Patton (*10*) compared gamma-

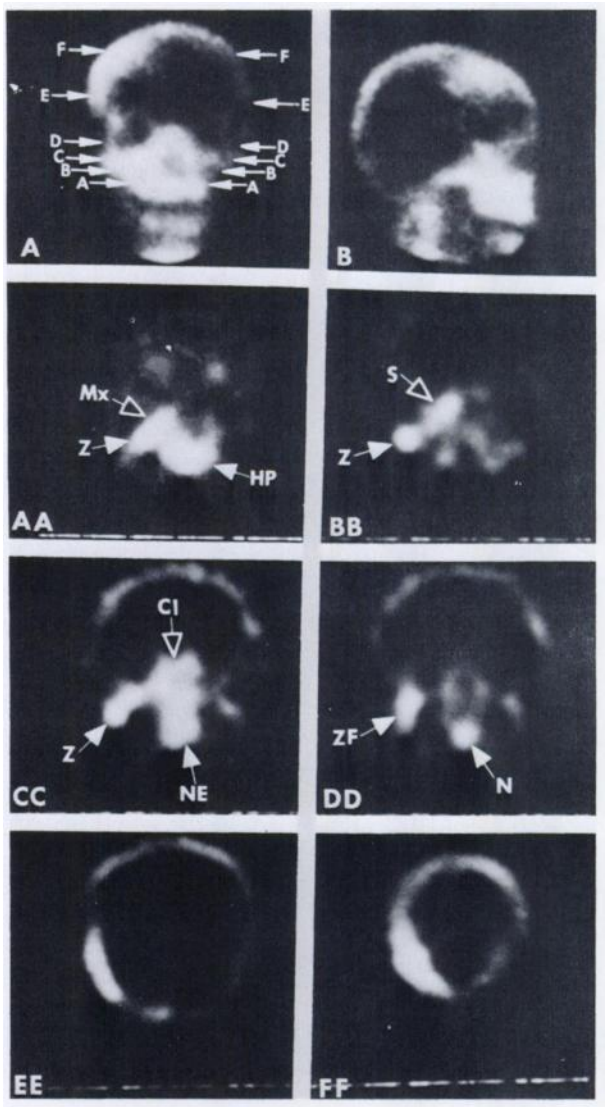

FIG. 5. Case 2. Histiocytic lymphoma. (A) Conventional anterior view showing levels of selected sections. (B) Conventional lateral. (AA–FF) Reconstructed tomograms. (Mx) maxilla; (Z) zygoma; (HP) hard palate; (S) body of sphenoid; (CI) clivus; (NE) nasoethmoid region; (ZF) zygomatic-frontal process; (N) nasion.

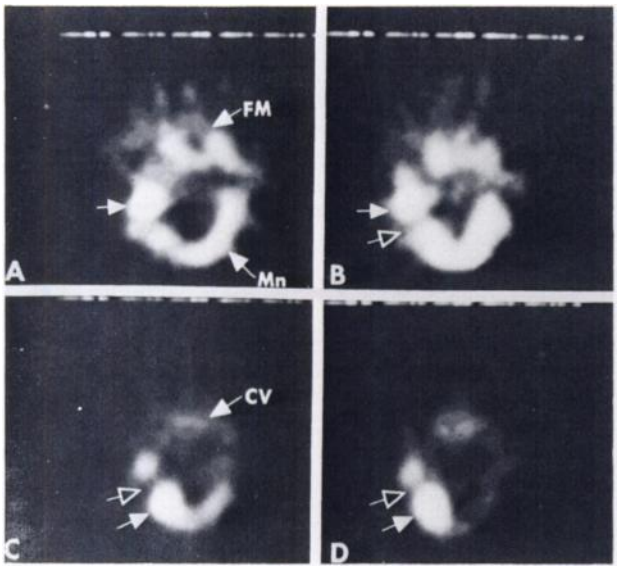

FIG. 6. Case 3. Squamous-cell carcinoma. Contiguous sections through mandible. Unlabeled open arrows point to photon-deficient lesion. Unlabeled closed arrows point to adjacent reactive bone. (FM) foramen magnum; (Mn) mandible; (CV) cervical vertebra.

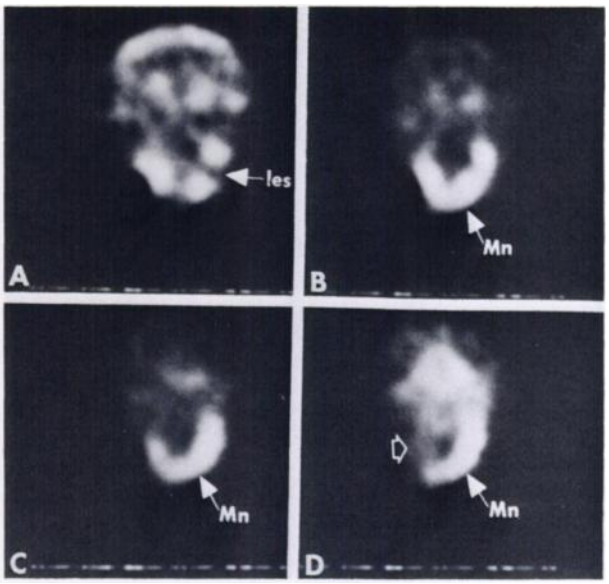

FIG. 8. Case 4. Osteoradionecrosis. Contiguous sections through mandible at successively lower levels. (les) Necrotic lesion; (Mn) mandible, showing reactive bone. Unlabeled open arrow points to decreased uptake in right side of mandible secondary to prior radiation therapy.

camera images of facial bones with radiographs and described the normal scintigraphic anatomy of the facial bones. In a study of maxillary-facial abnormalities, Gates and Goris (*1*) also discuss the anatomy of the bones of the face. They studied various scanning positions using a dried skull with a thallium-201 flood source and correlated this with the technetium-99m phosphate bone scans in 88 patients with diseases of the facial bones. The various projections used included lateral, oblique lateral, anterior, modified Waters, and Waters views. Each projection was useful in defining some portion of the skull with the exception of the Waters view, which produced difficulties due to facial foreshortening. They conclude that interpretation from any single view may be difficult or misleading, and they advocate that for the most complete examination, six views be obtained: both laterals, both lateral obliques, anterior, and a modified Waters.

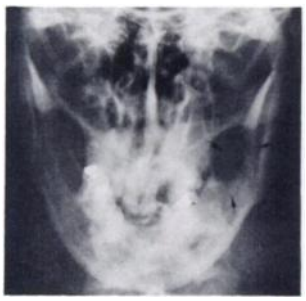

FIG. 7. Case 3. Radiograph of jaw showing lytic lesion in right mandible in area corresponding exactly to photon-deficient lesion seen in tomograms, cf. Fig. 6.

It is clear from these presentations that even with multiple projections, the exact anatomic extent of disease is often difficult to define. In any projection, deep structures may remain hidden by the superficial. Theoretically, emission transaxial tomography should provide accurate reconstructions of the anatomy of the bones of the face, with the distinct advantage of allowing separation of the deep from the superficial structures. Only one anecdotal report of emission bone tomography has appeared in the literature in an article by Kuhl et al. (*11*), defining the utility of the Mark IV system for tomography of the brain.

Using the Humongotron, a single-photon emission tomograph, we were able to study patients without evidence of facial disease to define the normal anatomy, and also to study a group of patients in whom abnormalities have been proven.

The use of a single-photon system has several distinct advantages. All patients were studied following routine skeletal imaging with a standard, widely available agent, technetium-99m pyrophosphate. The system uses a standard gamma-camera detector* mounted on a rotational device and is interfaced to a small on-line computer†. The time for both data acquisition and processing (20–30 min) is approximately the same as the time required to do a series of static views of the face, as suggested by Gates and Goris.

Emission computed tomography is a useful technique. In our study, the normal and abnormal transaxial anatomy was clearly defined. The tomograms revealed information that was not available from either the routine bone scan or from x-ray studies. It offers particular advantages in problem areas, such as bone scanning of the face and skull, where the complex structures of the mandible and facial bones are easily studied and well defined.

ACKNOWLEDGMENTS

This work was supported by USPHS Grant GM-22678.

The authors would like to gratefully acknowledge the assistance of Dr. Thomas M. Oelrich of the University of Michigan, Department of Anatomy for his help in supplying and reviewing anatomical material and Pamela Pietras for editorial and secretarial assistance.

FOOTNOTES

* Searle Radiographics Pho/Gamma HP.

† Medical Data Systems, Inc. "Trinary System".

REFERENCES

1. GATES GF, GORIS ML: Maxillary-facial abnormalities assessed by bone imaging. *Radiology* 121: 677–682, 1976

2. KEYES JW, ORLANDEA N, HEETDERKS WJ, et al: The Humongotron—a scintillation camera transaxial tomograph. *J Nucl Med* 18: 381–387, 1977

3. GAMBARELLI J, GUERINEL G, CHEVROT L, et al: *Computerized Axial Tomography*. New York, Springer-Verlag, 1977, pp 31–98

4. EYCLESHYMER AC, SCHOEMAKER DM: *A Cross-Section Anatomy*. New York, Appleton Century Crofts, 1970, pp 3–33

5. WOODBURNE RT: *Essentials of Human Anatomy*. New York, Oxford University Press, 1961, pp 149–260

6. ARFT SC: Radioisotope bone scanning as a diagnostic aid relative to bone lesions of the jaws. Masters Thesis, Horace H. Rackham School of Graduate Studies, The University of Michigan, 1975, pp 1–34

7. GARCIA DA, TOW DE, JANSONS D, et al: Jaw imaging in clinical dental diagnoses. *J Nucl Med* 18: 604, 1977 (Abst)

8. OLSON WH, MCCOMBS RK: Positive (^{99m}Tc) diphosphonate and ^{67}Ga-citrate scans in ameloblastoma: Case Report. *J Nucl Med* 18: 348–349, 1977

9. ALEXANDER JM, ALAVI A, HANSELL JR: Bone imaging in evaluation of jaw lesions. *J Nucl Med* 16: 511, 1975 (Abst)

10. JONES BE, PATTON DD: Bone scans of the facial bones: Normal anatomy. *Amer J Surg* 132: 341–345, 1976

11. KUHL DE, EDWARDS RQ, RICCI AR, et al: The Mark IV system for radionuclide computed tomography of the brain. *Radiology* 121: 405–413, 1976